Portugaliae Electrochimica Acta 2019, 37(2), 83-91

DOI: 10.4152/pea.201902083

PORTUGALIAE ELECTROCHIMICA ACTA
ISSN 1647-1571

Shatavari (*Asparagus Racemosus*) as Green Corrosion Inhibitor of Aluminium in Acidic Medium

Sumayah Bashir,[a] Garima Singh,[a] Ashish Kumar[b,*]

[a] *Department of Chemistry, School of Physical Sciences, Lovely Professional University, Punjab, India*
[b] *Department of Chemistry, School of Civil Engineering, Lovely Professional University, Punjab, India*

Received July 20, 2016; accepted June 15, 2017

Abstract

Plant extracts containing heteroatoms can be used as corrosion inhibitors as they are non-polluting, cheap and eco-friendly. The present work focuses on Asparagus Racemosus (Shatavari) as a corrosion inhibitor of aluminium in acidic medium. The techniques that have been used include weight loss method, quantum chemical analysis and scanning electron microscopy. It was seen that at 4000 ppm concentration of inhibitor the corrosion inhibition efficiency was 72.28%. The inhibition efficiency increased with increase in concentration. The best description of adsorption isotherm was seen to follow Langmuir adsorption isotherm. In order to elucidate the reactivity and molecular structure of inhibitor, quantum chemical parameters were utilized. The surface properties of the metal specimen were determined by SEM.

Keywords: Corrosion, weight loss, HOMO, LUMO, HCl, asparagus racemosus, inhibition efficiency.

Introduction

Aluminium plays a pivotal role in automobiles, packaging, utensils, pipelines etc. In relation to corrosion, one of the most affected sectors is petroleum industry, metal industry, shipping segment, leading to major economical and resource loss [1]. Aluminium has a protective oxide layer over its surface which acts as an added advantage against corrosion. This aluminium oxide layer is, however, amphoteric in nature and thus, in highly acidic or basic medium it gets dissolved. This breakdown of protective oxide layer exposes bare metal surface for corrosion, therefore making it necessary to investigate methods for mitigation of corrosion in aluminium.

Aluminium metal (in the bare, protective oxide layer free form) once exposed to the electrolyte undergoes corrosion. The reaction corresponding to the presence of chloride ions in the medium is:

* Corresponding author. E-mail address: drashishchemlpu@gmail.com

$$[Al\ (OH)]^{+2} + Cl^{-} \leftrightarrow [Al\ (OH)\ Cl]^{+}$$

Since the order of the reaction obtained is three, thus a soluble complex [Al (OH) Cl] Cl will be formed:

$$[Al\ (OH)]^{+2} + 2Cl^{-} \leftrightarrow [Al(OH)Cl]Cl$$

Formation of this soluble complex ion leads to an increase in the deliquescence of metal which depends on the concentration of chloride ions. Thus, we can say, with the increasing concentration of HCl, an increase in the corrosion rate is observed [2-3].

Large numbers of organic compounds have been used as corrosion inhibitors. Mostly, the compounds containing heteroatoms like O, N, S in their structure are thought to be efficient in preventing corrosion of Al in many inhibitors, a lot of them having been used, e.g., imidazoline derivatives [4], capparis decidua [5], delonix regia extract [6], gongronima latifolium extract [7], Bismarck brown eye [8], methyl orange [9], onion extract [10], hibiscus rosa-Sinesis [11], etc. These inhibitors have numerous N, O and S containing alkaloids which get adsorbed onto the metal surface which basically hinder the release of H^{+} and disintegration of metal ions. Steroidal Saponin-Shatavarin (I-IV) and Sarsasapogenin are the active constituents of Asparagus Racemosus. The structure of these constituents is given below:

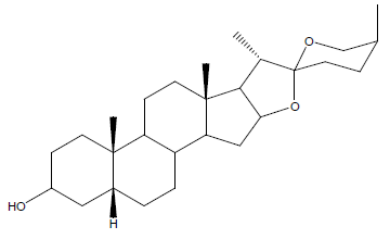

Sarsasapogenin

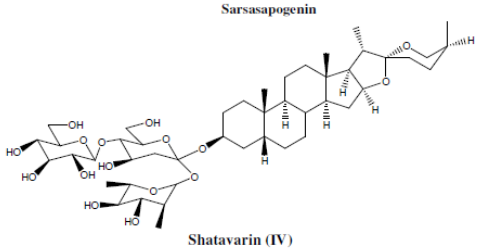

Shatavarin (IV)

Inhibition efficiency of corrosion inhibitors increases with increase in concentration of active components as well as it is directly proportional to the number of electron withdrawing or electron donating groups present in the inhibitor [12]. Presence of heteroatoms, polar functional groups and π-electrons as active centers in a particular compound makes it an effective corrosion inhibitor [13-15] because these heteroatoms or π-electrons facilitate electronic interactions between metal and inhibitor, which in turn helps in the adsorption of inhibitor onto the metal surface [16]. Increase in environmental awareness has raised the demand of green, non-toxic, cheap and environmentally friendly corrosion inhibitors [17-19].

Experimental

Materials

Aluminium coupons having chemical composition 0.35% Fe, 0.25% Si, 0.05% Cu, 0.05% Zn, 0.03% Mg, 0.03% Mn, 0.03% Ti and remainder Al have been utilized.

Weight loss method

The dimensions of aluminium coupons used were 2 x 2.5 x 0.1 cm. Before performing the experiment the coupons were abraded with emery papers of grade nos. 100, 220 and 400, and then washed with distilled water and acetone. The weight loss of polished and dried aluminium coupons was ascertained by weighing the metal coupon before and after immersing in 100 cc of 1 M HCl in absence (blank) and presence of inhibitor. The percentage inhibition efficiency was calculated using the following formula:

$$\eta\% = W0 - Wi/W0 \times 100 \qquad (1)$$

where, W0 = weight loss in the blank solution, Wi = weight loss in the presence of the inhibitor at the said concentration.

Quantum chemical analysis

Quantum substance examination was performed utilizing the MNDO and AM1 technique for the quantum chemical package MOPAC 6.0 of Hyperchem 7.5. The algorithm utilized for calculation was Polak-Rieberre, which is quick and precise. The accompanying parameters were (E_{HOMO}), (E_{LUMO}), energy band gap, $\Delta E = E_{HOMO}-E_{LUMO}$, binding energy, heat of formations and the dipole moment (μ).

SEM analysis

For SEM analysis, the aluminium coupons were immersed in 100 mL of 1 M HCl in the presence and absence of optimum concentration of the two inhibitors, separately, for 1 hr. Then they were removed, rinsed quickly (with sodium bicarbonate, water and acetone) and dried. The surface morphology of the metal coupons was determined and recorded using Scanning electron microscope.

Results and discussion

Weight loss studies

Separately weight loss studies with respect to concentration of inhibitor, time of immersion and temperature, have been carried out. As the temperature was increased, the corrosion inhibition efficiency was also seen to increase. Table 1 summarizes the effect of inhibitor concentration on the corrosion inhibition efficiency. The maximum efficiency of 74.4% is seen at the inhibitor concentration of 6000 ppm. All these results are observed at 298 K. The increase in inhibition efficiency with the increase in concentration is because of the increased adsorption coverage of aluminium caused by the addition of the inhibitor.

Table 1. Inhibition efficiency (η %) of asparagus racemosus on aluminium at 298 K.

S. No.	Acid(M) Inhibitor (ppm)	W0 (g)	Wi (g)	W0-Wi(g)	ɵ	Ƞ%
1	1M	0.3778	0.1873	0.1905	NA	NA
2	1000	0.3736	0.2728	0.1008	0.470866	47.08661
3	2000	0.3733	0.3052	0.0681	0.64252	64.25197
4	3000	0.3727	0.3174	0.0553	0.709711	70.97113
5	4000	0.3778	0.325	0.0528	0.722835	72.28346
6	5000	0.3771	0.328	0.0491	0.742257	74.22572
7	6000	0.3712	0.3225	0.0487	0.744357	74.4357

It was seen that increase in temperature leads to decrease in inhibition efficiency. The inhibition efficiency was seen at the temperatures varying from 288 to 303 K at the inhibitor concentration of 4000 ppm. As the temperature increases, the corrosion rate also increases leading to the decrease in inhibition. The corrosion of metal in acidic medium is typically joined by the evolution of H_2 gas; increase in temperature fastens the corrosion rate resulting in higher dissolution of the metal [20]. Table 2 gives the estimations of inhibition efficiency and surface coverage at various temperatures.

Table 2. Inhibition efficiency and surface coverage of asparagus racemosus on aluminium at different temperatures.

S. No	Temp (K)	Inhibitor concentration (ppm)	Initial Wt. (g)	Final Wt. (g)	Weight loss (g)	ɵ	$^{\eta}$ (%)
1	303	Blank (1 M)	0.3786	0.0228	0.3558	NA	NA
		Shatavari (4000)	0.3714	0.256	0.1154	0.67566	67.56605
2	298	Blank (1M)	0.3795	0.054	0.3255	NA	NA
		Shatavari (4000)	0.3715	0.2812	0.0903	0.722581	72.25806
3	293	Blank (1M)	0.3709	0.1196	0.2513	NA	NA
		Shatavari (4000)	0.3718	0.3128	0.059	0.765221	76.52209
4	288	Blank (1M)	0.3769	0.1672	0.2097	NA	NA
		Shatavari (4000)	0.3734	0.3326	0.0408	0.805436	80.54363

Adsorption study

In order to comprehend the interaction of inhibitor particles and the metal surface, adsorption isotherms can be utilized. The estimations of surface coverage relating to concentrations of inhibitor are utilized to get the best straight adsorption fit isotherm. The most generally utilized adsorption isotherms are Langmuir and Freundlich ones. Equations (2) and (3) represent such isotherms.

Langmuir isotherm, $$\frac{\theta}{1-\theta} = K_{ads}C \qquad (2)$$

Freundlich isotherm, $$\theta = K_{ads}C \qquad (3)$$

K_{ads} stands for the adsorption equilibrium constant, Ɵ is the surface coverage and C defines the concentration of inhibitor in ppm. Fig. 1 gives the Langmuir adsorption isotherm. Slope of C/Ɵ vs. C gives a straight line with slope almost

equal to 1, suggesting the adsorption of inhibitor on aluminium surface follows Langmuir adsorption isotherm [21].

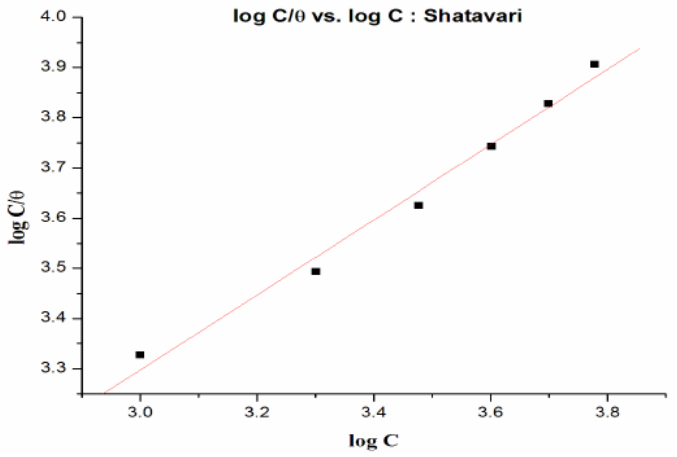

Figure 1. Langmuir adsorption isotherm in 1 M HCl at 298 K with asparagus racemosus as corrosion inhibitor of aluminium.

Thermodynamic activation parameters were elucidated based on the temperature dependence of corrosion rate by Arrhenius equation:

$$C_R = A \exp\left(\frac{-E_a}{RT}\right) \qquad (4)$$

where E_a is the apparent effective activation energy, R is the general gas constant, C_R is the corrosion rate. The enthalpy of activation was calculated by using Eyring equation:

$$\ln\frac{C_R}{T} = \left(-\frac{\Delta H}{R}\right).\frac{1}{T} + \left(\frac{\ln R}{Nh} + \frac{\Delta S}{R}\right) \qquad (5)$$

where, h is the Planck´s constant, N is the Avogadro's number, ΔH is the enthalpy of activation and ΔS is the entropy of activation.

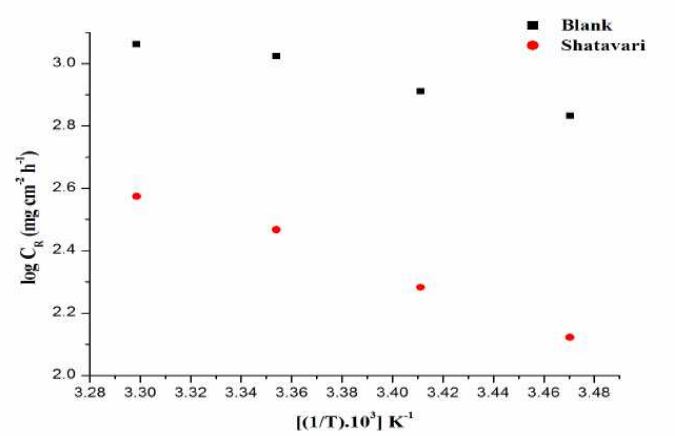

Figure 2. Arrhenius plot of log C_R vs. 1000/T for aluminium in 1 M HCl in presence (optimum concentration of 4000 ppm) and absence of inhibitor.

A plot of log C_R versus 1000/T gave a straight line, as appeared in Fig. 2. The estimations of activation energy acquired from the slope of lines are recorded in Table 3. Fig. 3 demonstrated the plot of log CR/T versus 1000/T. Straight lines were acquired with a slant of (- ΔH/R) and intercept of [(ln(R/Nh) + (ΔS/R)] from which estimations of ΔH and ΔS are ascertained. Examination of Table 3 demonstrated that values of Ea measured for the solution containing the inhibitor are greater than in blank HCl. Elevation in Ea determines either physical adsorption or decline in the adsorption of inhibitor particles on aluminum as a result of increase temperature [20].

The endothermic nature of reaction was demonstrated by the positive value of ΔH. Estimations of ΔS show the ordering of inhibitor atoms on the surface of metal [22].

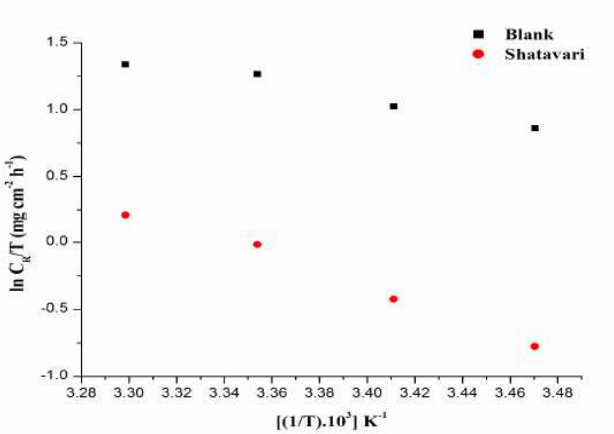

Figure 3. Arrhenius plot of log C_R /T vs. 1000/T for aluminium in 1 M HCl in presence (optimum concentration of 4000 ppm) and absence of inhibitor

Table 3. Thermodynamic parameters in the presence and absence of the inhibitor.

S. No.	Inhibitor	ΔH_{ads} (kJ mol^{-1})	ΔS_{ads} (J K^{-1} mol^{-1})	Ea (kJ mol^{-1})
1	Blank	24.36526	-105.78	26.82782654
2	Shatavari	49.06025	-33.6424	51.52534206

Mechanism of adsorption

The interaction of metal and the inhibitor is based on the mechanism of inhibition. Mechanism of adsorptions gives us an idea about the metal electron interaction with the protective inhibitor molecules. Aluminium is considered to be positively charged in HCl with respect to the potential zero charge. Hence, inhibitor exists as neutral molecule in acidic solution. Fig 4 elucidates the donor-acceptor interaction between unshared electrons of the heteroatom and the vacant p orbital of aluminium metal.

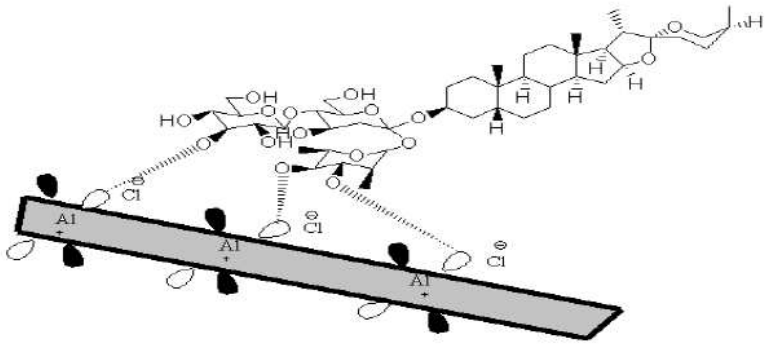

Figure 4. Adsorption behavior of inhibitor on the surface of aluminium.

Quantum chemical study

These estimations were performed so as to explore the process of adsorption and mechanism of inhibition examined for inhibitor molecule. The different optimized structures of inhibitor are given in Fig. 5. Keeping in mind the end goal to develop a molecular structure and reactivity of an inhibitor, it might be essential to concentrate on the properties that specifically impact the metal inhibitor interaction. Some of these parameters include energies of sub-atomic orbital, E_{HOMO}, E_{LUMO}, ΔE ($E_{LUMO} - E_{HOMO}$), and dipole moment. The estimation of these computed quantum compound parameters are given in Table 4. As E_{HOMO} indicates with electron donating capacity of a molecule, higher E_{HOMO} values are prone to demonstrate an inclination of molecule for donation of electrons to the acceptor molecule. Larger values of E_{HOMO} encourage adsorption by impacting the transport process through adsorbed layer. This way, the energy of E_{LUMO} demonstrates the capacity of an atom to accept electrons. At the lower E_{LUMO} values, the more likely is that the atom will accept electrons. Lower values of ΔE ($E_{LUMO} - E_{HOMO}$) propose higher corrosion inhibition efficiency because the energy required for removing the electron will be low [23]. Higher dipole moment proposes more adsorption and in this way higher inhibition efficiency because of more polarization [20].

Table 4. Quantum chemical parameters of *asparagus racemosus.*

Dipole Moment	8.022
E_{HOMO}	-8.834484 eV
E_{LUMO}	0.958921 eV
ΔE (E_{LUMO}-E_{HOMO})	9.793405 eV

SEM analysis

The morphology of the metal specimen was revealed by SEM. The micrographs in Fig. 6 (a, b, c) show the micrograph of polished aluminium coupon without immersion in either of the solutions, specimen in blank HCl and inhibitor solution, respectively. It is clear from the figure that (a) has large number of pits and cavities and also the surface is rough, whereas in case of (b) the pits are less and the surface is smooth, which is an evidence that inhibitor has formed a protective layer on the surface of the metal through adsorption [24].

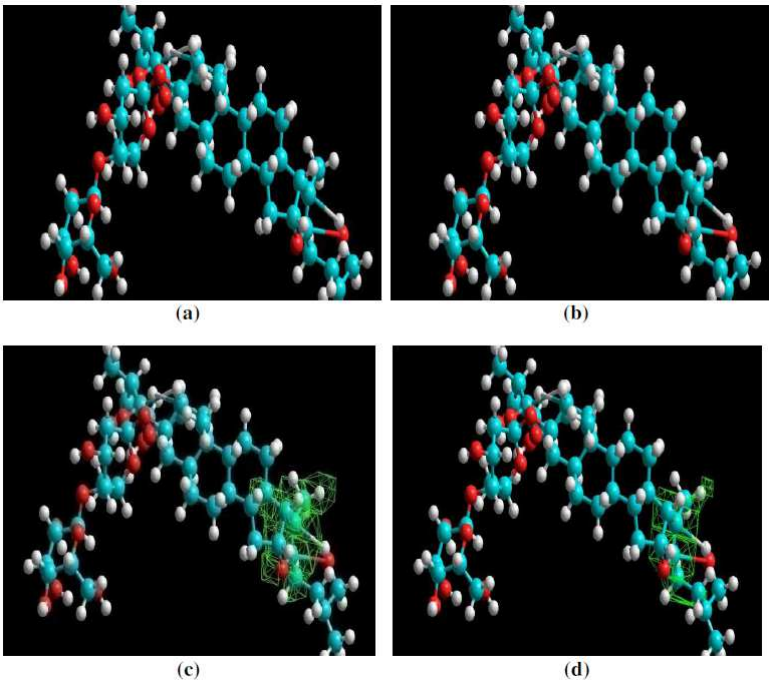

Figure 5. Quantum chemical structures of *asparagus racemosus.* (**a**) Geometry optimization. (**b**) Total charge density. (**c**) HOMO. (**d**) LUMO.

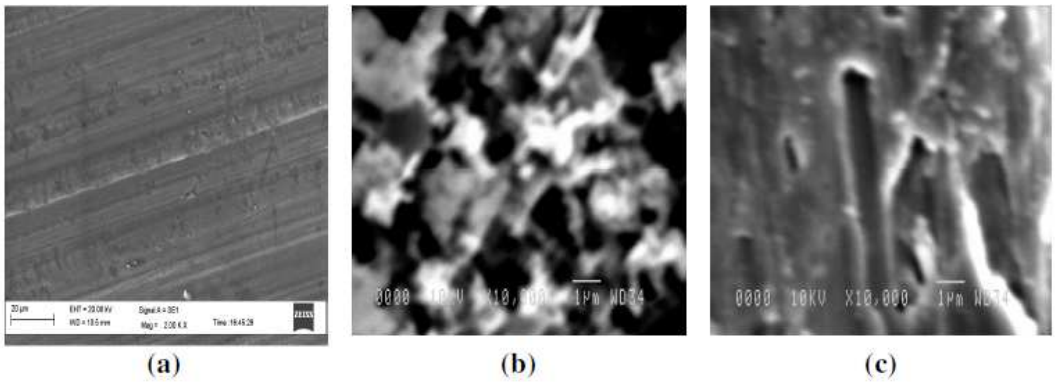

Figure 6. SEM micrographs of aluminium in 1 M HCl after 1 hr immersion time. (**a**) polished aluminium coupon, (**b**) blank 1 M HCl, (**c**) inhibitor (4000 ppm).

Conclusion

The results demonstrate that asparagus racemosus is an effective corrosion inhibitor of aluminium in acidic medium. The positive value of ΔH suggests that the reaction is endothermic and the rate of corrosion is slow. The adsorption of inhibitor on the surface of aluminium obeys Langmuir adsorption isotherm. The addition of inhibitor leads to increase in activation energy showing that the inhibitor is being physically adsorbed on the surface of the metal. Quantum compound approach is adequate to estimate the effectiveness of inhibitor utilizing hypothetical approach.

Acknowledgments
The authors are pleased to acknowledge Lovely Professional University (LPU) for providing the facilities for the research.

References

1. Hurlen T, Lian H, Odegard O, Valand T. Electrochim Acta. 1984;49:537.
2. Ford FP, Burstein GT, Hoar TP. J Electrochem Soc. 1980;127:127.
3. Nguyen TH, Foley RT. J Electrochem Soc. 1982;129:129.
4. Putilova IN, Balizin SA, Baranik VP. Met Corr Inhib Per. 1960;305.
5. JainT, Choudhary R, Mathur SP. Mater Corros. 2006;57:422.
6 Okafor PC, Ikpi ME, Uwah IE, et al. Corros Sci. 2008;50:2310.
7. Choudhary R, Jain T, Mathur SP. Bull Electrochem. 2004;20:67.
8. Sharma P, Upadhyay RK, Chaturvedi A, et al. JTR Chem. 2008;15:21.
9. Talati JD, Gandhi DK. Ind J Technol. 1991;29:227.
10. Dubey RS, Upadhyay SN. J Electrochem Soc India. 1944;74:143.
11. Rajendran S, Jeyasundari J, Usha P, et al. Port Electrochim Acta. 2009;27:153.
12. Verma C, Olasunkanmi LO, Ebenso EE, et al. J Phys Chem C. 120 2016;120:11598.
13. Quraishi MA, Ansari KR, Yadav DK, et al. Int J Electrochem Sci. 7 2012;7:12301.
14. Bousskri A, Anejjar A, Messali M, et al. J Mol Liq. 2015;211:1000.
15. Belghiti ME, Tighadouini S, Karzazi Y, et al. J Mater Environ Sci. 2016;7:319.
16. Geethamani P, Kasthuri PK. Cog Chem. 2015;1:1091558.
17. Majidi L, Znini M, Ansari A, et al. Int J Electrochem Sci. 2013;8:7381.
18. Elmouaden K, Chaouay A, Oukhrib R, et al. Int J Electrochem Sci. 2015;10:7955.
19. Gerengi H, Ugras HI, Solomon MM, et al. J Adh Sci Tech. 2016;1:1.
20. Yadav DK, Maiti B, Quraishi MA. Corros Sci. 2010;52:3586.
21. Hmamou DB, Salghi R, Zarrouk A, et al. Int J Ind Chem. 2012;3:25.
22. Quraishi MA, Danish J. Mat Chem Phys. 2003;78:687.
23. Belghiti ME, Karzazi Y, Tighadouini S, et al. J Mater Environ Sci. 2016;7:956.
24. Pandian BR, Sethuraman MG. Mater Lett. 2008;62:2977.